Journal of Applied Polymer Science

WILEY

Applied Polymer SCIENCE

RESEARCH ARTICLE

Gamma-Irradiated PVP-PVAL Clay-Hydrogels: Evaluations of Mechanical and Antibacterial Properties With Different Clay Concentrations

L. D. Almeida | K. O. Gonçalves | V. Parra | D. F. Parra

Nuclear and Energy Research Institute–IPEN/USP, São Paulo, SP, Brazil

Correspondence: D. F. Parra (dfparra@ipen.br)

Received: 2 October 2024 | **Revised:** 18 March 2025 | **Accepted:** 2 April 2025

Funding: This work was supported by CAPES (88887.854542/2023-00).

ABSTRACT

The pursuit of biomaterials and medicines dosed at therapeutic levels has become increasingly intensive over time. There is a growing need for materials that respond more efficiently to the demands of daily use. Hydrogels have the potential to meet this demand due to the specific characteristics of their reagents and synthesis methods. This article investigates the influence of Laponite RD (Lap), a clay material, as a crosslinking mediator in the gamma radiation synthesis of PVP/PVAL hydrogels. The central question addressed is how Lap, which possesses dual properties as both a drug carrier and a crosslinking mediator, can enhance both functionalities without antagonistic effects. The data presented in this study demonstrate the interaction between polymers and clay, as confirmed by FTIR, XRD, and TG/DSC analyses. Swelling and gel fraction tests revealed that the polymer network is also altered by the presence of Lap. Mechanical resistance tests indicated that the Young's modulus varies with increasing Laponite concentration, in addition to enhancing the elasticity of the hydrogel. However, despite these findings, all analytical techniques suggest that there may be a limit to the polymer–clay interaction. Furthermore, the hydrogels did not exhibit an inhibition halo against *E. coli* bacteria, but positive optical density results indicated bacterial inhibition. Additionally, this research contributes to the future development of a matrix suitable for clay-drug systems, in hydrogel form, for drug delivery systems in pharmaceutical applications.

1 | Introduction

Polymeric three-dimensional networks are widely recognized and studied, particularly after undergoing polymeric crosslinking. Among these networks, those capable of absorbing and retaining large volumes of water, as well as exchanging biological fluids, are referred to as hydrogels. These hydrogels possess exceptional properties that make them suitable for a variety of applications, including pharmaceutical uses [1], agricultural applications for reducing fertilizer and pesticide usage, cosmetics and personal care products [2, 3], the removal of organic and inorganic pollutants [4], and biomedical applications such as tissue engineering. Their ability to mimic extracellular matrix environments, promote wound healing, and serve as membranes in drug delivery systems makes them particularly valuable in the biomedical field [5, 6].

The ability of hydrogels to exchange biological fluids, facilitated by the water contained within their three-dimensional networks, allows them to be engineered to respond to external stimuli. Such hydrogels are classified as "smart hydrogels." They can undergo significant changes in response to variations in environmental conditions, such as temperature, pH, ionic strength, salt type, solvent composition, light, magnetic or electric fields, and ultrasound. These stimuli trigger the release of drugs encapsulated within the hydrogel. This functionality is made possible

by the hydrogel's ability to alter its sol fraction without compromising its gel structure, which instead undergoes dimensional changes such as swelling or shrinking. This unique behavior also enables applications in bioseparation processes for molecules and proteins [7].

To design hydrogels that respond to specific internal or external stimuli, it is essential to develop a polymeric network tailored to the intended requirements. The properties of the polymer network determine how the material will react to changes, whether by absorbing contaminated fluids or releasing therapeutic agents [8, 9]. Notably, the response speed of hydrogels is a critical factor in determining their efficiency for a given application.

Since the late 1960s, the synthesis of hydrogels for biomedical applications using ionizing radiation has seen significant advancements. Dr. Rosiak and colleagues from Łódź Technical University proposed an innovative approach to initiate crosslinking through the use of ionizing radiation in dilute aqueous solutions. This method is conducted in a pure polymer-solvent system, eliminating the need for additives such as monomers, catalysts, or crosslinking agents. This approach offers considerable advantages, particularly for biomedical applications, as it allows simultaneous synthesis and sterilization of the product. The radiation-based method is reproducible, versatile, and cost-effective [10].

One potential approach to enhancing the mechanical properties of hydrogels is the incorporation of clays into their composition. Clays are natural or synthetic, fine-grained, earthy materials that exhibit plasticity when moistened with water, making them suitable for a wide range of applications [11] Among these, montmorillonite (MMT) clays have been extensively utilized in nanocomposites [12] MMT clays can be obtained either naturally or synthetically, and their lamellar structure facilitates exfoliation through both physical and chemical processes [13]. Several studies have reported that the addition of small amounts (< 10%) of organophilic clays can significantly enhance the mechanical, thermal, and barrier properties, as well as the dimensional stability of nanocomposites [14]. For instance, nanodispersed clay has been used to improve the thermal stability and increase the hardness of biopolymers [15].

Laponite, a synthetic clay with a structure similar to the natural mineral Wyoming hectorite, has been widely studied as an additive in hydrogels. Previous research [15, 16] has characterized Laponite as an ideal synthetic clay that, when dispersed in water, self-assembles into a viscoelastic and thixotropic material. In our earlier study, we demonstrated the synthesis of PVP/PVAL hydrogels crosslinked with clay using gamma radiation, which resulted in improved mechanical properties of the hydrogel [17]. Additionally, our group showed, using the FESEM technique, modifications in the morphology of the irradiated blend PVA/PVP containing Laponite in comparison with clay added separately to each polymer. The results indicated a more homogeneous morphology with smaller pores in the combination of PVA/PVP/Laponite as the crosslink effect of the radiation.

In another study researchers have synthesized Laponite-based hydrogel membranes using alginic acid sodium salt and PVA, specifically for wound dressing applications. These membranes, containing 2% by weight of Laponite, exhibited reduced swelling capacity and degradation rates, along with significantly enhanced mechanical properties [18]. Such hydrogel membranes are particularly useful as dressings for drug delivery systems in topical applications.

The incorporation of clay as a drug carrier offers additional advantages, such as the ability to modulate drug release in such systems. Therefore, the primary objective of this work was to develop PVAL/PVP hydrogels incorporating Laponite clay and to investigate the effects of varying clay concentrations (0%, 1%, 2%, 3%, 5%, 8%, and 12% by weight). By characterizing the physical, mechanical, and microbiological properties, including bacterial inhibition, this study aims to elucidate the influence of Laponite on the performance of these hydrogels in various applications. Additionally, this research contributes to the future development of a matrix suitable for clay-drug delivery systems in biomaterials.

2 | Materials and Methods

2.1 | Materials

Laponite RD (LP) from BKY Additives & Instruments (BR) from 1% to 12% (w/w of polymer), Poly Vinyl Alcohol (PVAL Mw 9000–10,000, 80% hydrolyzed) and Poly Vinyl Pyrrolidone (PVP K90, Mw 1200 kDalton) from Êxodo Científica, Agar (Mw = 100,000) from Oxoid, and Polyethylene glycol (PEG 400) from Brenit AG were used in the formulation of hydrogels synthesis in membrane format of 8 × 15cm. The water used was distilled.

2.2 | Hydrogel Synthesis

For the preparation of the hydrogels, the reagents were added in stages. First, the mix of 8.0 g of PVAL and 3.0 g of PEG was stirred in aqueous solution. After dissolution, 8.0 g of PVP was added, followed by the Laponite, and finally the Agar (2.0 g), raising the temperature of the solution to 85°C for 5 min. After completing the dissolutions, the solution was placed in plastic trays and sent to Gamma radiation at a rate of 25 kGy and a dose rate of 5.5 kGy.h^{-1}.

2.3 | Characterization of Hydrogels

2.3.1 | Gel Fraction

The determination of the gel fraction was obtained from pieces of hydrogel, weighing about 2 g for each sample. The pieces were placed in stainless steel cages (500 mesh) and immersed in boiling water inside flasks connected to a reflux distiller for 4 h. After that, the extracted samples were dried in an oven at 60°C until a constant mass was achieved. The gel fraction of the material was calculated using Equation (1), with the system adapted to the standard (ASTM D 2765). The gel fraction indicates the insoluble part, whose value is assigned to the crosslinked polymeric fraction.

$$Gel\ fraction\ (\%) = \frac{(mf - mi)}{mi} \times 100 \quad (1)$$

where "mi" is the mass of the dry sample before extraction and "mf" is the final mass of the sample after extraction and drying.

2.3.2 | Swelling

Swelling tests in distilled water were performed in triplicates for the hydrogels. The samples were weighed and placed in beakers containing 10 mL of distilled water and kept at room temperature. The samples were weighed every hour for a total period of 7 h, and after these intervals, they were weighed between 24 and 50 h. To perform the weighing, the samples were removed from the beaker and dried with paper towels to remove excess water from the surface. The amount of water absorbed, expressed as a percentage, was determined by Equation (2).

$$S = \frac{(Ws - Wo)}{Wo} \times 100\,\% \quad (2)$$

where "S" is water absorption, "Ws" is the weight of the swollen sample, and "Wo" is the weight of the initial gel sample.

2.3.3 | Spectroscopy in the Infrared Region—FTIR

The FTIR spectra of the synthesized hydrogels were obtained in ALPHA Bruker equipment, operating in the range of 4000–600 cm^{-1}.

2.3.4 | X-Ray Diffraction—XRD

The X-ray profile was obtained using a Bruker D2 PHASER diffractometer, operating at 30 kV and with a current of 10 mA, varying 2θ from 5° to 40°, with an integration time of 1 s and radiation from Cu 1.5408 Å.

2.3.5 | Strength Tests

Stable Micro System texturometer, model TATX2i, performed the Tension tests according to ASTM D 882–95 standard, using specimens measuring 80 × 30 × 2.5 mm, in triplicate under tensile speed of 90 mm/min^{-1}, using a load cell capacity of 10 N_2. To carry out the test, the sample was fixed in one claw model A/TGT and submitted to draw at a speed of 0,8 $mm.s^{-1}$ based on the initial distance (lo), up to break. The stress–strain curves were plotted, and mechanical properties of elastic modulus and tensile strength were estimated.

2.3.6 | Differential Scanning Calorimetry—DSC

DSC analyzes used the Mettler-Toledo DSC 822 apparatus. Sealed aluminum crucibles containing 7 mg of sample, under an inert atmosphere of N_2, were heated following the program of: Initial heating from 20°C to 250°C; then cooling from 250°C to 20°C and reheating from 20°C to 250°C with a flow rate of 10°C/min^{-1}.

2.3.7 | Thermogravimetry—TG

TG/DTG analyzes used the Mettler-Toledo DSC 822 apparatus. The samples were heated in alumina pans of 40 μL containing 7 mg of sample, under an inert atmosphere of N_2 at 10 mL/min^{-1} and programmed to decompose in the temperature interval of 20°C to 600°C.

2.3.8 | In Vitro Antibacterial Activity

2.3.8.1 | Culture of *E. coli*. The culture of *E. coli* W3110 grew in Luria–Bertani broth (LB) for 18 h at 37°C overnight. It was transferred into an LB medium and maintained until the exponential growth phase. The bacterial suspensions at 10^8 CFU/mL were then prepared by adjusting the optical density to $OD_{620\,nm} = 0.200 \pm 0.005$.

2.3.9 | Antibacterial Activity of Hydrogels

The disk diffusion test in agar and antimicrobial activity test proved the antibacterial effect of hydrogels on the viability of *E. coli*. Pieces of hydrogels of ~10 mm in diameter performed the disk diffusion tests in agar using as positive control Ampicillin (0.1 g/mL) and incubation of the plates in an oven at 30°C for 24 h. After incubation on the agar plate, the discs were washed off using 1 mL of sodium chloride saline solution (0.9%). The calculation of optical density used the values of measurement at 620 nm.

3 | Results and Discussion

3.1 | Gel Fraction Determination

The hydrogels were synthesized by modifying only the concentration of Laponite present in each one of them. The synthesis of the hydrogel was carried out by gamma radiation in 60Co gamma rays at 25 kGy. Crosslinking induced by ionizing radiation proved to be a suitable method for hydrogel synthesis [19, 20]. The results presented in Figure 1 show that the hydrogel without the Laponite showed a gel fraction of around 87%. With the presence of Lap at concentrations of 1%, 2%, 3%, and 5%, the gel fraction increased as expected, but for the high concentrations, 8% and 12%, the gel fraction decreased. These data show that Laponite has interacted with the polymer crosslinked network and is acting as a secondary linking agent, modifying its crosslinking density [21]. It is possible to notice that there exists a limit for a Lap interaction due to a decrease in gel content for Laponite's high concentration (8% and 12%). The gel fraction results can be corroborated with the Swelling results since the higher the Gel Fraction, the greater the entanglement of the polymer chains, thus affecting their elasticity capacity to absorb hydrophilic fluids [22].

3.2 | Swelling Test

Regarding the degree of swelling, an important aspect of hydrogels is used for drug delivery. The results presented in Figure 2

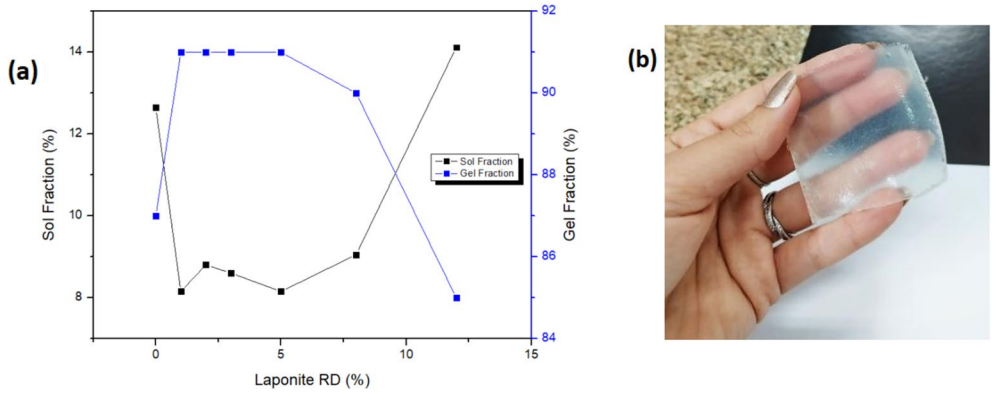

FIGURE 1 | Analysis of the hydrogels: (a) gel fraction and soluble fraction for the samples with different concentrations of Laponite and (b) image of the hydrogel with 12% Laponite. [Color figure can be viewed at wileyonlinelibrary.com]

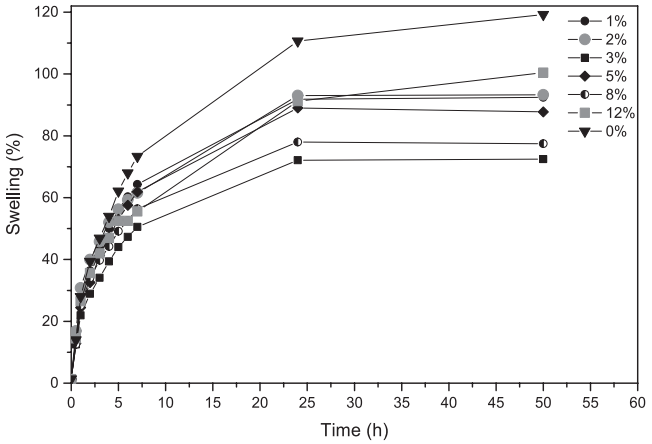

FIGURE 2 | Swelling behavior as a function of time in contact with water, of hydrogels PVAL/PVP and PVAL/PVP/clay Laponite, obtained by gamma irradiation at 25 kGy.

demonstrate that all hydrogels absorb water over the first 10 h, corroborating with the previous study in the literature [9]. It can be highlighted that the hydrogel with the highest percentage of Lap (12%) also showed good absorption, raising its degree of swelling close to the hydrogel without the presence of Laponite.

The swelling behavior is associated with several factors that influence the recombination of radicals formed by radiolysis in the hydrogel, such as, for example, the interactions of clay with polymers, functional groups along the polymeric chain, and with ionization species [23]. The result of 0% of Laponite, as a reference, could be evidence that the clay interferes with crosslinking density due to the high swelling behavior as mentioned above and confirmed by the increase in Gel Fraction. The crosslinking density directly affects the amount of water absorbed; therefore, only 2% and 12% did not achieve the expected behavior. This result may indicate that the high concentration should alter the expected crosslinking agent properties of the clay.

3.3 | FTIR Spectroscopy

To confirm the chemical structures of the synthesized hydrogels, FTIR spectroscopy was carried out. Figure 3 shows the spectra of hydrogels from 0% to 2% (a), from 3% to 12% (b) and reagents (c). Nevertheless, the spectra have showed a possible overlap of bands between the 990 and 1003 of the polymers and Laponite, as shown in Figure 4; these bands refer to the stretching (C—O), stretching (C—N) and (Si—O—Si) bonds for PVP, PVAL, and Laponite, respectively. The bonds highlighted in the spectra in Figure 3 show a broad peak at around 3500–3200 cm^{-1} indicating —OH groups; stretching at 2923 cm^{-1} from PVAL; C═O at 1660 cm^{-1}, characteristic of PVP; C—H_2 at 1247 cm,$^{-1}$ and Si—O_2 at 840 cm^{-1} referring to Laponite. The peaks at 1730 and 1250 cm^{-1} disappeared due to covalent interaction between PVA and PVP. The peak at 1660 cm^{-1} of PVP decreases in intensity while the peak at 1005 cm^{-1} increases in intensity with the Lap concentration increases [24–26].

The broader peak at 995 cm^{-1} attributed to Si—O—Si stretching of the Lap, in Figure 4, is displaced to 1005 cm,$^{-1}$ indicating the interaction of the clay with the irradiated polymers. Figure 5 illustrates the spectra of the hydrogels (0%–12%) and their increase in intensity at a wavelength of 1097 cm^{-1} in relation to the $[SiO^{(4-2x)-}_{4-x}]_n$ silicates found with the addition of the clay [24]; these compounds may have been formed as a result of radiolysis from the gamma radiation used for polymer crosslinking, where, after previous exfoliation, the Laponite modified the polymer structure to form a new interaction by crosslink combination. As previously shown, Laponite has a Si—O—Si structure around 995 cm; thus^{-1}, the hydroxyl group present in PVAL and the PVP ketone are likely to interact during irradiation with Si—O— by hydrogen bond formation.

3.4 | XRD

The XRD profile of the hydrogels with and without clay was obtained using the XRD technique, together with the diffractions of the reagents: PVAL, PVP, and Laponite, as shown in Figure 6. Figure 7 allows evaluating the interaction between Laponite and polymer.

Figure 6 shows the profile of the main reagents used in the synthesis of the hydrogels (PVP, PVAL and LP). There are approximate angles among the three of 2θ: 19.6°, 19.6°, and 20.1°, for Lap, PVAL, and PVP, respectively. When studying Laponite

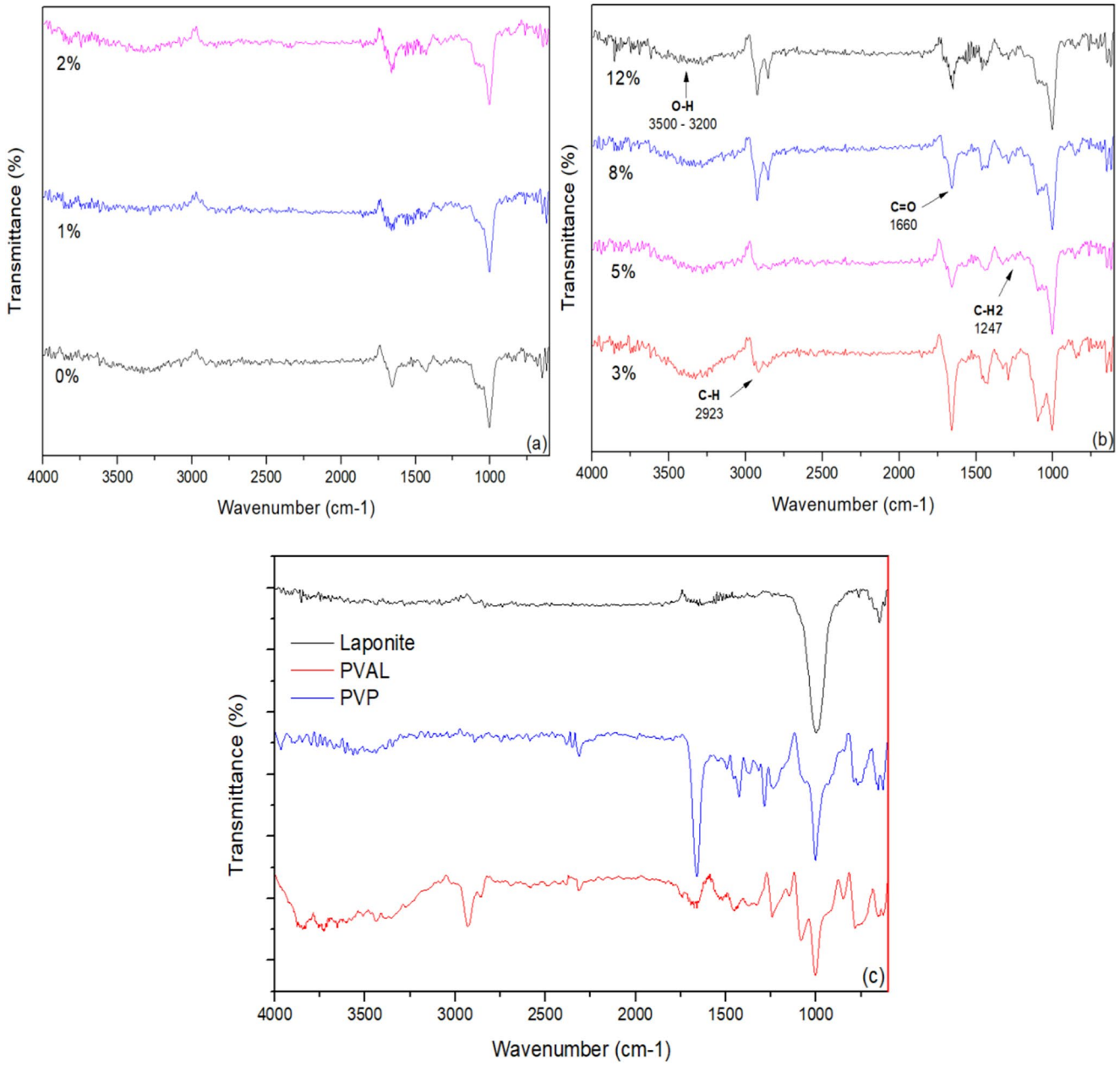

FIGURE 3 | (a) 0%, 1%, and 2%; (b) 3%, 5%, 8%, and 12%; (c) Reagents. Hydrogel FTIR spectra of samples of different concentrations from 0% to 12% of Lap and FTIR of the main components of the formulation. [Color figure can be viewed at wileyonlinelibrary.com]

in particular, the visualization of its peaks after irradiation should be taken seriously since its presence can show a problem with the dispersion of the reagent and, when exfoliated, the profile should not show any peaks related to it. The 2θ peaks: 19.57°, 27.70°, and 34.91° can be related to their basal and flat spacing (hkl), as shown in the following: d(100) = 4.53247 Å, d(005) = 3.21788 Å, and d(110) = 2.56804 Å [27].

Meanwhile, Figure 7 shows a relationship between the concentrations of 0%, 1%, and 2% (a) and 3%, 5%, 8%, and 12% (b). It is possible to see a predominant peak around 19°–20° with small variations between them; these angles, as shown in Figure 6, are derived from both polymers and laponite, with greater intensity for PVAL. As discussed in the literature, when the clay lamellae are exfoliated, the XRD profiles do not show any peaks, so it is noticeable that there is a broad band between the angles of 25° and 35°, which could be a peak shift caused by the Laponite not being completely exfoliated and only a distancing of the lamellae by swelling; another reason why Laponite may not exfoliate completely is due to the strong ionic bonding present in Laponite's structure, where, if there is an excess or difficulty in adsorbing Laponite to the polymer chains, exfoliation will not take full place [21, 28].

At the same time, Figure 8 observes one difference in intensity at angles 2θ between 5° and 10°, where Laponite appears with a significant signal in the 12% sample, while others show no intensity; this confirms the presence of Laponite that does not exfoliate in the 12% concentration in the polymer matrix.

From the diffraction curves, the crystallinity rate of each hydrogel was calculated, which is presented in Table 1.

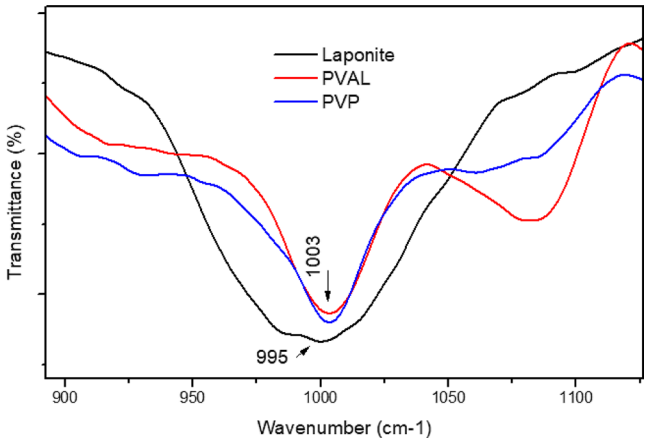

FIGURE 4 | Comparative spectra of reagents in the interval of 900–1000 cm^{-1}. [Color figure can be viewed at wileyonlinelibrary.com]

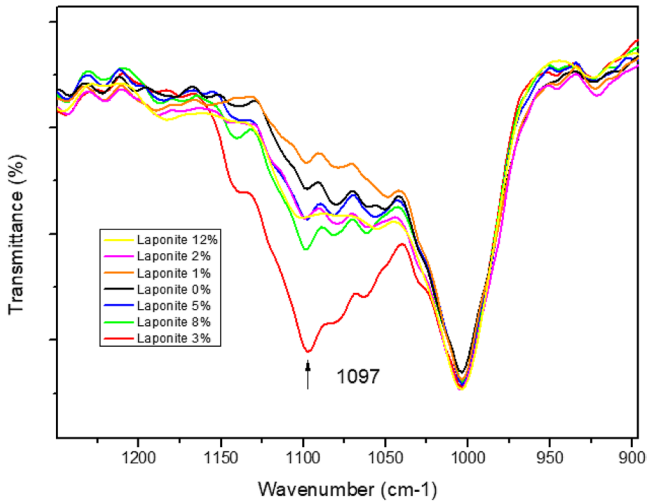

FIGURE 5 | Hydrogels spectra with evidence of silicates observed at 1097 cm^{-1}. [Color figure can be viewed at wileyonlinelibrary.com]

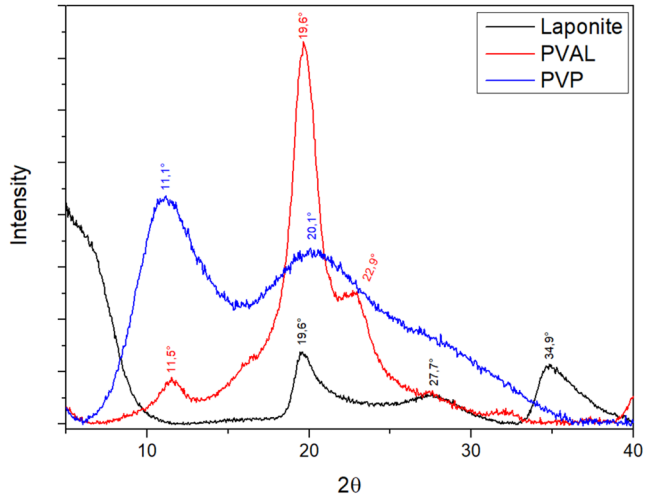

FIGURE 6 | XRD of the hydrogel main components: PVA, PVP, and Laponite. [Color figure can be viewed at wileyonlinelibrary.com]

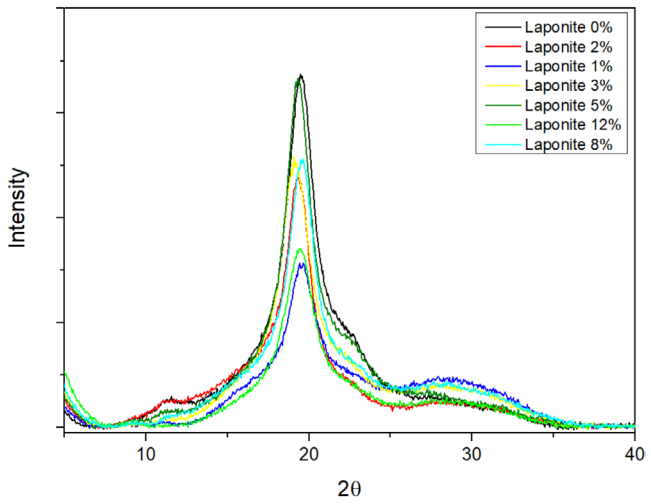

FIGURE 7 | XRD profile of hydrogels with different Laponite concentrations from 0% to 12%. [Color figure can be viewed at wileyonlinelibrary.com]

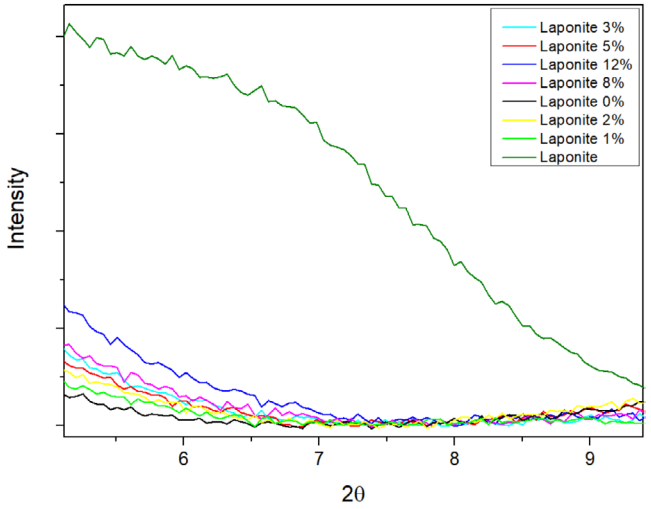

FIGURE 8 | Hydrogel and Laponite XRD of 2θ between 5° and 10°. [Color figure can be viewed at wileyonlinelibrary.com]

TABLE 1 | Crystallinity % of each hydrogel with and without Laponite.

Samples (%Lap)	Crystallinity (%)
0	39,8
1	52,5
2	58,7
3	62,0
5	59,7
8	58,4
12	70,4

From the crystallinity values obtained for the hydrogels via XRD, it can be concluded that Laponite acts as a nucleating agent and increases the crystallinity of the material. These data show that its incorporation increases this property, but there is a noticeable limit between 1% and 8% with an average of 58.26%; however, the increase in the sample's crystallinity from 12% to

70.38% is because Laponite is saturated in the polymer network and still contributes to the material's crystallinity. This may complement the XRD profiles shown in Figure 7.

3.5 | Differential Scanning Calorimetry

DSC analysis is an important method to determine physical and chemical changes such as phase transitions, crystallinity temperature (Tc) and melting parameters (Tm). It was decided to analyze the hydrogel samples in the following temperature range: 20°C–250°C at a heating rate of 10°C/min^{-1}, under nitrogen atmosphere, with three runs with the objective of showing the Tc and Tm. Figure 9 presents the results obtained from the second run (Tc) for all membranes, and Figure 10 shows the third run (Tm). Table 2 presents the specific results of Tm and Tc and their respective T_{onset} and T_{endset}.

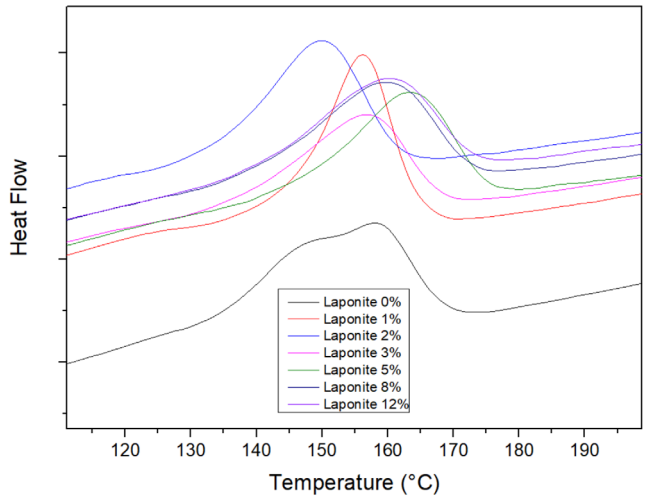

FIGURE 9 | The crystallinity peak of the second run in DSC curve of hydrogels with and without Laponite. [Color figure can be viewed at wileyonlinelibrary.com]

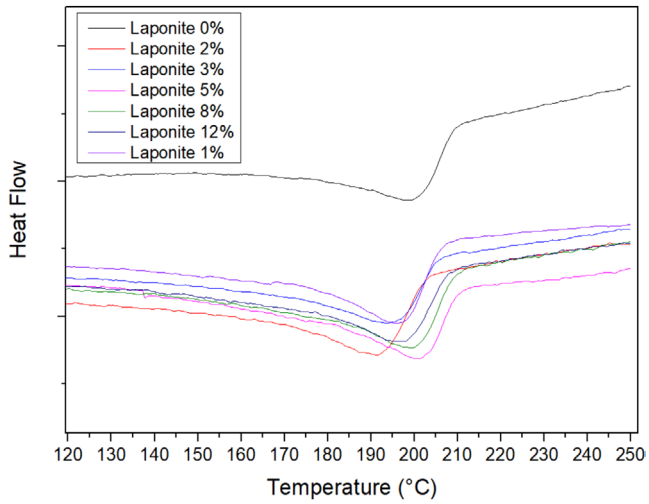

FIGURE 10 | The melt (third run) DSC curve of hydrogels with and without Laponite. [Color figure can be viewed at wileyonlinelibrary.com]

There is a notable change in the profile of the crystallization peak between the samples with and without Laponite. Although the changes are not too significant, it can be seen from the Tonset and Tendset results that there is a narrowing of the peak in the second run, which may mean an increase in the ordering

TABLE 2 | DSC Tm and Tc values of hydrogels with 0%–12% of Laponite.

Lap samples (%)	Crystallization Tc (°C)			Melting temperature Tm (°C)		
	T_{onset}	T_{endset}	Peak	T_{onset}	T_{endset}	Peak
0	169	135	158	172	209	200
1	168	140	156	189	207	198
2	162	133	150	171	202	191
3	168	136	157	170	205	194
5	175	146	164	179	209	200
8	173	139	160	174	199	209
12	173	141	160	184	207	198

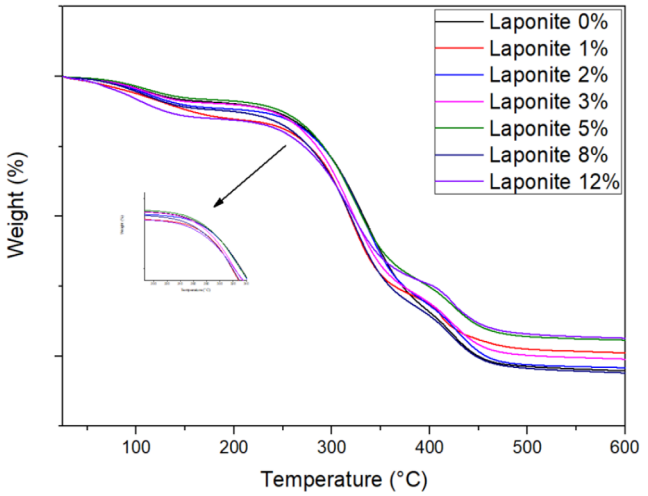

FIGURE 11 | TG curves for hydrogel membranes of PVAL/PVP, PVAL/PVP/Laponite 0%–12% of Laponite. [Color figure can be viewed at wileyonlinelibrary.com]

TABLE 3 | TG Tonset and Tendset of all hydrogels of different laponite concentrations.

Samples (%)	T_{onset} (±1°C)	T_{endset} (±1°C)
0	289	375
1	291	354
2	292	370
3	294	358
5	295	362
8	283	359
12	289	359

of the crystalline chains and the action of Laponite as a nucleating agent. These data corroborate those evaluated in the XRD section. With regard to melting, both the profile and the peak changed very little and there were no significant changes in this property.

3.6 | Thermogravimetry Analysis

The samples characterized by TG were the hydrogels in all concentrations of Laponite and the polymers that form the crystalline network PVP and PVAL. The samples were previously dried to eliminate most of the water present in their network. Figure 11 and Table 3 show the data of all hydrogels synthesized.

Figure 11 shows three events: the first one relates to the decomposition of wet materials, the second to PVAL, and the third to PVP [9, 29]. In the data above, it can be seen that the concentration of Laponite did not significantly interfere with the thermal properties of the hydrogels, being mainly visualized in the T onset values; however, the T endset values showed a decrease that indicates a faster decomposition of the hydrogels in this second event, being explained by the preferential interaction of Laponite with the PVAL chain forming hydrogen bonds Si—OH [9]. Although there was no significant change in weight loss of the PVP/PVA and Laponite-loaded membrane, the thermal degradation temperature of the mixed matrix membrane was much higher than that of the pure membrane due to the Laponite addition into the PVA matrix. This fact is associated with the interaction of PVA and Laponite as a secondary crosslinker.

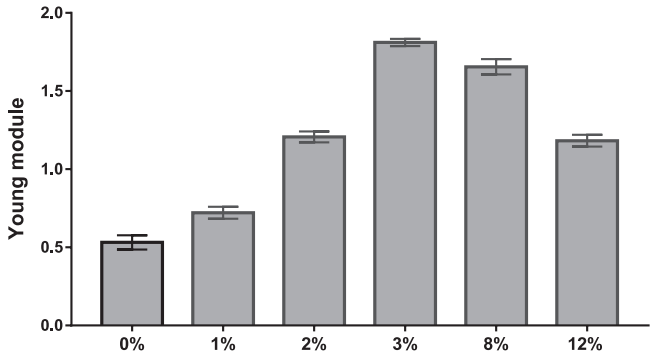

FIGURE 12 | Young's modulus calculated for membranes with Laponite.

3.7 | Strength Test

Concerning the tensile strength and elongation of the hydrogels, it was obtained directly from the curves of the 0%, 2%, 3%, 8%, and 12% concentrations; as shown in Figure 12 data for the 5% concentration were not possible, as there were not enough samples. All the hydrogels showed some tensile strength and modulus of elongation until rupture. When the results are compared, the hydrogels without Laponite show greater elastic deformation, but when Laponite is present in the composition, it increases the modulus of the force supported by the hydrogel, creating an effect of resistance to deformation of the hydrogel. The explanation for this behavior is that Laponite can alter the density of crosslinks and decrease the elastic property [30, 31]. This is what happens with hydrogel samples with 3% Laponite. These results show that there is a clay–polymer interaction, and that this interaction promotes an improvement in the modulus of the hydrogels. The synthesized hydrogels are homogeneous, with no fracture points or Laponite aggregates.

The curves presented show the rheological behavior of the hydrogels, which have tensile strength that improves until a limit concentration. Laponite improves the resistance, helping to increase the tensile modulus, confirming that there is a Laponite/polymer interaction. Therefore, Laponite did not show results for strain increase; on the contrary, at 1%, 2%, and 3% it showed a decrease, which shows the greater crosslinking of the polymer chain.

Figure 12 shows the stress × strain relationship of the material in Young's Modulus. This property is important for understanding the concept of material stiffness and its mechanical behavior as resistant hydrogels. The concentration of 3% showed the highest stiffness, followed by 8% and 12%, even though these were

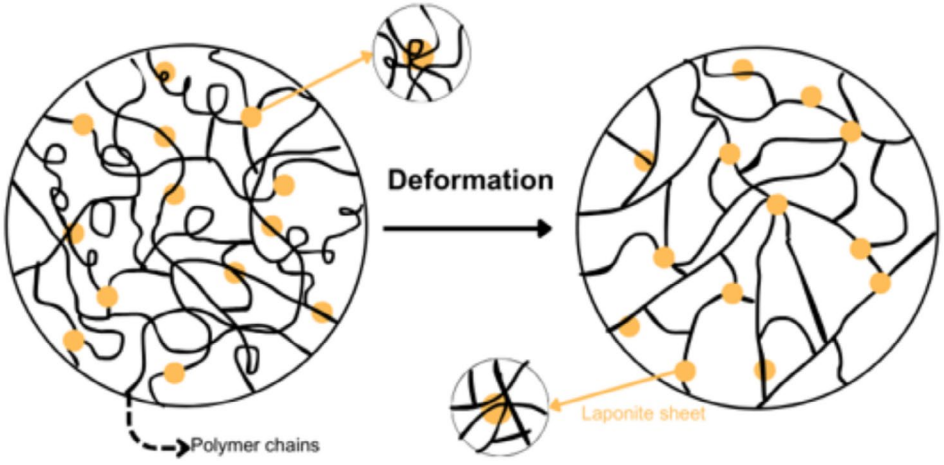

FIGURE 13 | Schematization of the possible arrangements of the Laponite clay lamellas in the polymer chains after their exfoliation. This representation shows how Laponite clay acts after swelling and deformation of polymer chains. No scale. [Color figure can be viewed at wileyonlinelibrary.com]

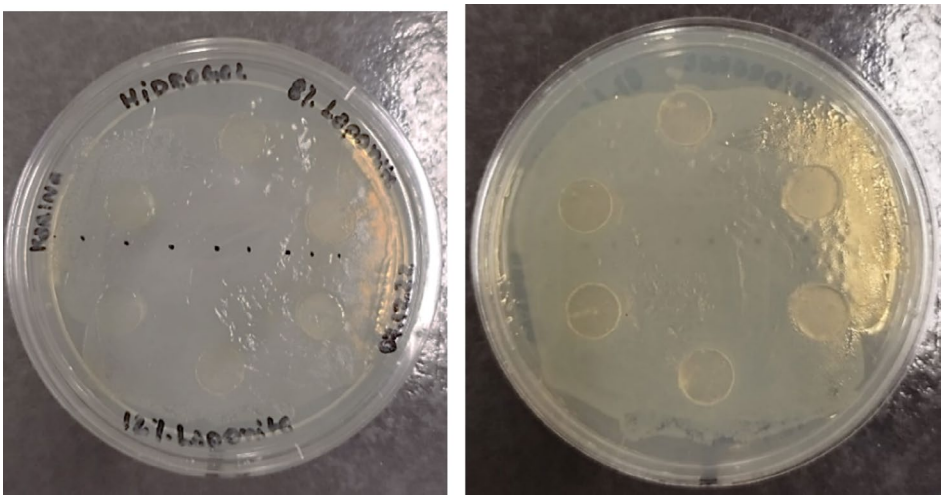

FIGURE 14 | Agar plates with *E. Coli* and hydrogels cut into 10 mm diameter discs with 8% and 12% Laponite in their composition, incubated for 24 h in an oven at 30°C. [Color figure can be viewed at wileyonlinelibrary.com]

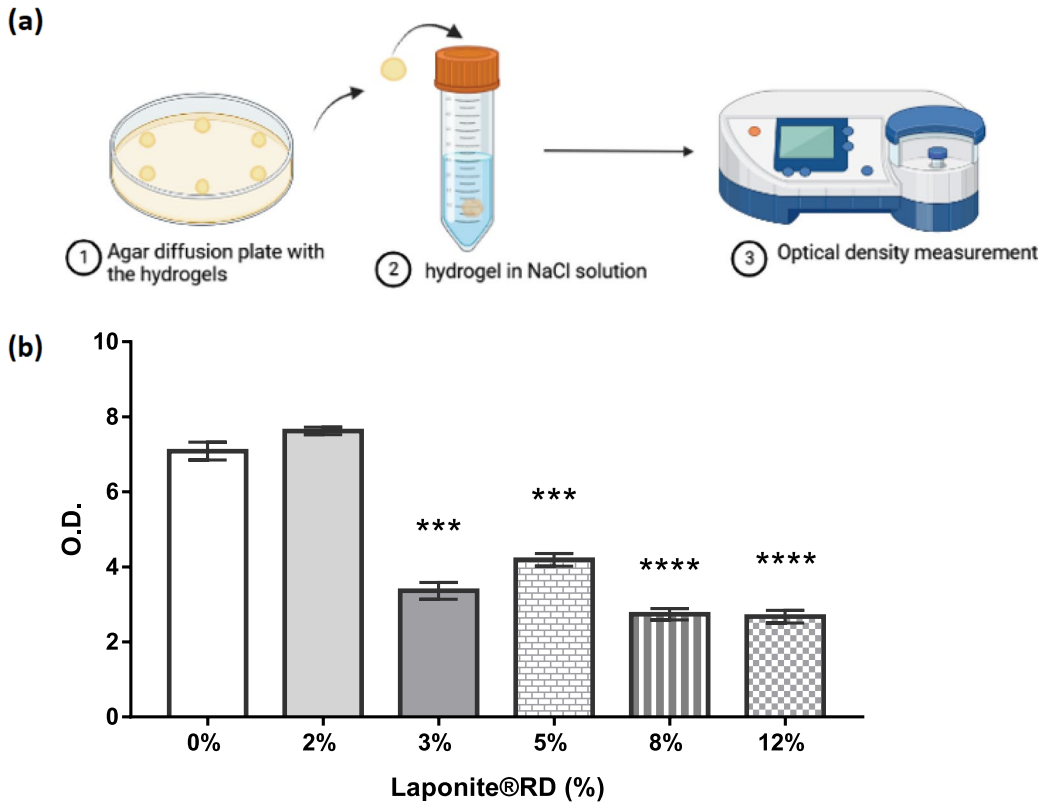

FIGURE 15 | Antibacterial activity of the hydrogels: (a) Scheme for obtaining the solution of bacteria grown in the hydrogel after incubation time in an oven (24 h and 30°C) and (b) results obtained in relation to the optical density measured after washing the hydrogels with NaCl solution (0.9%). Data were compared using the ANOVA test followed by the Dunnett test with p values: **** < 0.0001. [Color figure can be viewed at wileyonlinelibrary.com]

higher than 0%, 1%, and 2%. These data contribute to up to a certain limit, in the case of 3%, above which Lap does not act as a crosslinker of more polymer chains.

Figure 12 shows the stress × strain relationship of the material in Young's Modulus. This property is important for understanding the concept of material stiffness and is a complement to understanding the mechanical behavior of hydrogels. The concentration of 3% showed the highest stiffness, followed by 8%, even higher than 0%, 1%, and 2%; these data contribute to proving that Lap acts by increasing the crosslinking density.

Laponite articulation within the hydrogel's three-dimensional network is due to the interaction of its lamellae with the polymer chains. Figure 13 shows a schematic of how Laponite is supposedly arranged between the three-dimensional network before and during mechanical deformation, where the polymer chains are aligned.

3.8 | Antibacterial Activity of Hydrogels

The antibacterial activity of the hydrogels was tested by the agar diffusion method. The hydrogels did not show a halo of bacterial growth relative to inhibitory activity (Figure 14). Other studies have shown similar results in hydrogels without drug in their composition [32].

As there were no results with the agar diffusion method, it was decided to perform a second analysis, in which each piece of hydrogel was washed in a NaCl solution to assess whether there was bacterial growth on its surface. Figure 15a presents the procedure of removal and hydrogel solution followed by optical density measurement (OD). Figure 15b represents the OD test results obtained.

The results obtained after the OD measurements showed that the hydrogels without clay or with a low concentration (2%) did not inhibit the growth of bacteria on their surface or in their surroundings. However, when the concentration of Laponite RD increases, the optical density decreases, revealing that in a way, the clay interferes with the proliferation of bacteria on the hydrogel surface, reducing the measured density by half of the value. The results reported a surface structural alteration in the crosslinked membranes, probable by smaller pores formation [17], when Lap is added. It makes difficult for the bacteria to grow, an environment that hinders bacterial growth, indicating favorable antibacterial activity.

4 | Conclusion

The process of synthesizing hydrogels with higher Laponite RD using gamma radiation from 60Co, at a 25 kGy dose, was reported. The clay was incorporated into the polymers, contributing to changes in the properties of the hydrogels. In addition, the effects of increasing the concentration of clay in the hydrogels on changes in the mechanical, biological, and physical characteristics of the hydrogels were studied. The Gel Fraction and Swelling results showed changes in the crosslink density of the hydrogels with high Laponite content; FTIR and XRD confirmed the interaction of Laponite with the polymer and the increase of PVA/PVP crystallinity. The DSC results indicated changes in the crystallization temperature. According to the results, the Laponite incorporated into the irradiated polymers acts as a nucleating agent, modifying the hydrogel properties and promoting network stability predictable and useful in hydrogels for drug delivery systems (DDS). However, it is possible to state that there is a concentration limit to the incorporation of Laponite in the gel, assuring its mechanical stability. Taking all the data into account, it is consistent to consider that the addition of clay between 3% and 8% in relation to the mass of the polymer is ideal for obtaining better hydrogel properties. At those concentrations, the clay is exfoliated.

Despite all the modifications in the polymer structure, clay hydrogels were not able to inhibit *E. coli* bacteria using the agar diffusion test for halo formation; however, the decrease to 50% of the optical density demonstrated a bactericidal effect. Therefore, this material can be considered a vehicle for transporting drugs to wounds for healing with a bactericidal activity.

Author Contributions

L. D. Almeida: writing – original draft (equal), writing – review and editing (equal). **D. F. Parra:** supervision (lead), writing – review and editing (supporting). **K. O. Gonçalves:** writing – original draft (equal), writing – review and editing (supporting). **V. Parra:** visualization (lead), writing – review and editing (equal).

Acknowledgments

The authors thank the CAPES funding agency and the Multipurpose Gamma Irradiation Facility—CETER/IPEN. Lucas D. Almeida thanks CNPQ for grants, project n° 88887.854542/2023-00.

Conflicts of Interest

The authors declare no conflicts of interest.

Data Availability Statement

The data that support the findings of this study are available from the corresponding author upon reasonable request.

References

1. S. Morariu, M. Bercea, L. M. Gradinaru, I. Rosca, and M. Avadanei, "Versatile Poly (Vinyl Alcohol)/clay Physical Hydrogels With Tailorable Structure as Potential Candidates for Wound Healing Applications," *Materials Science and Engineering: C* 109 (2020): 110395, https://doi.org/10.1016/j.msec.2019.110395.

2. W. E. Rudzinski, A. M. Dave, U. H. Vaishnav, S. G. Kumbar, A. R. Kulkarni, and T. M. Aminabhavi, "Hydrogels as Controlled Release Devices in Agriculture," *Designed Monomers and Polymers* 5, no. 1 (2002): 39–65, https://doi.org/10.1163/156855502760151580.

3. S. Mitura, A. Sionkowska, and A. Jaiswal, "Biopolymers for Hydrogels in Cosmetics," *Journal of Materials Science: Materials in Medicine* 31, no. 6 (2020): 1–14, https://doi.org/10.1007/s10856-020-06390-w.

4. M. Song, S. Wang, J. He, D. Kan, K. Chen, and J. Lu, "Synthesis of Hydrogels and Their Progress in Environmental Remediation and Antimicrobial Application," *Gels* 9, no. 16 (2023): 1–24, https://doi.org/10.3390/gels9010016.

5. H. Yu, X. Xu, X. Chend, T. Lu, P. Zhang, and X. Jing, "Preparation and Antibacterial Effects of PVA-PVP Hydrogels Containing Silver Nanoparticles," *Journal of Applied Polymer Science* 103, no. 1 (2007): 125–133, https://doi.org/10.1002/app.24835.

6. M. J. A. Oliveira, D. F. Parra, V. S. Amato, and A. B. Lugão, "Hydrogel Membranes of PVA/Clay by Gamma Radiation," *Radiation Physics and Chemistry* 84 (2013): 111–114, https://doi.org/10.1016/j.radphyschem.2012.06.035.

7. J. J. Kim and K. Park, "Smart Hydrogels for Bioseparation," *Bioseparation* 7, no. 4 (1998): 177–184.

8. H. L. Lim, Y. Hwang, M. Kar, and S. Varghese, "Smart Hydrogels as Functional Biomimetic Systems," *Biomaterials Science* 2, no. 5 (2014): 603–618, https://doi.org/10.1039/c3bm60288e.

9. M. J. A. Oliveira, *Doctoral Thesis, Obtenção de Membranas de Hidrogéis Para Tratamento Alternativo da Leishmaniose Tegumentar* (Universidade de São Paulo, 2013).

10. T. S. Balogh, E. Bonturim, E. L. D. Vieira, A. B. Lugao, and S. Kadlubowski, "Synthesis of Poly(N-Vinyl Pyrrolidone) (PVP) Nanogels by Gamma Irradiation Using Different Saturation Atmospheres," *Radiation Physics and Chemistry Ogh* 198 (2022): 110238, https://doi.org/10.1016/j.radphyschem.2022.110238.

11. K. Haraguchi, "Nanocomposite Hydrogels," *Current Opinion in Solid State and Materials Science* 11, no. 3–4 (2007): 47–54, https://doi.org/10.1016/j.cossms.2008.05.001.

12. C. Yao, Z. Liu, C. Yang, et al., "Poly (N-Isopropylacrylamide)-Clay Nanocomposite Hydrogels With Responsive Bending Property as Temperature-Controlled Manipulators," *Advanced Functional Materials* 25, no. 20 (2015): 2980–2991, https://doi.org/10.1002/adfm.201500420.

13. L. Rodrigues, A. Figueiras, F. Veiga, et al., "The Systems Containing Clays and Clay Minerals From Modified Drug Release: A Review," *Colloids and Surfaces B: Biointerfaces* 103 (2013): 642–651, https://doi.org/10.1016/j.colsurfb.2012.10.068.

14. R. Barbosa, E. M. Araújo, L. F. Maia, O. D. Pereira, T. J. A. Melo, and E. N. Ito, "Morfologia de Nanocompósitos de Polietileno e Poliamida-6 Contendo Argila Nacional," *Polímeros* 16 (2006): 246–251, https://doi.org/10.1590/S0104-14282006000300016.

15. N. Willenbacher, "Unusual Thixotropic Properties of Aqueous Dispersions of Laponite RD," *Journal of Colloid and Interface Science* 182, no. 2 (1996): 501–510, https://doi.org/10.1006/jcis.1996.0494.

16. Y. M. Joshi, G. R. K. Reddy, A. L. Kulkarni, N. Kumar, and R. P. Chhabra, "Rheological Behavior of Aqueous Suspensions of Laponite: New Insights Into the Ageing Phenomena," *Proceedings of the Royal Society A* 464 (2008): 469–489, https://doi.org/10.1098/rspa.2007.0250.

17. M. J. A. Oliveira, V. J. Santos, L. F. Freitas, A. B. Lugão, and D. F. Parra, "Poly(Vinyl Alcohol) (PVAl) and Poly(N-2-Vinyl-Pyrrolidone) Hydrogels Nanostructured by Laponite Clay for Drug Delivery," *Journal of Materials Science and Engineering* 12 (2022): 97–107, https://doi.org/10.17265/2161-6221/2022.7-9.003.

18. N. Golafshan, R. Rezahasani, M. T. Esfahani, M. Kharaziha, and S. N. Khorasani, "Nanohybrid Hydrogels of Laponite: As a Potential Wound Healing Material," *Carbohydrate Polymers* 176 (2017): 392–401, https://doi.org/10.1016/j.carbpol.2017.08.070.

19. M. C. F. C. Felinto, D. F. Parra, C. C. Da Silva, J. Angerami, M. J. A. Oliveira, and A. B. Lugão, "The Swelling Behavior of Chitosan Hydrogels Membranes Obtained by UV- and γ-Radiation," *Nuclear Instruments and Methods in Physics Research Section B: Beam Interactions With Materials and Atoms* 265, no. 1 (2007): 418–424, https://doi.org/10.1016/j.nimb.2007.09.025.

20. A. T. Zafalon, V. J. Santos, F. Esposito, et al., "Synthesis of Polymeric Hydrogel Loaded With Antibiotic Drug for Wound Healing Applications," in *Characterization of Minerals, Metals, and Materials*, ed. B. Li, J. Li, S. Ikhmayies, et al. (Springer, 2018), https://doi.org/10.1007/978-3-319-72484-3_18.

21. F. Xie, C. Boyer, V. Gaborit, et al., "A Cellulose/Laponite Interpenetrated Polymer Network (IPN) Hydrogel: Controllable Double-Network Structure With High Modulus," *Polymers* 10, no. 6 (2018): 1–18, https://doi.org/10.3390/polym10060634.

22. R. N. Richbourg, A. Ravikumar, and N. A. Peppas, "Solute Transport Dependence on 3D Geometry of Hydrogel Networks," *Macromolecular Chemistry and Physics* 22, no. 16 (2021): 1–7, https://doi.org/10.1002/macp.202100138.

23. Z. Tadmor and C. G. Gogos, *Principles of Polymer Processing* (John Wiley & Sons, 2006).

24. G. R. Mahdavinia, S. Ettehadi, M. Amini, and M. Sabzi, "Synthesis and Characterization of Hydroxypropyl Methylcellulose-g-Poly (Acrylamide)/LAPONITE RD Nanocomposites as Novel Magnetic- and pH-Sensitive Carriers for Controlled Drug Release," *RSC Advances* 5, no. 55 (2015): 44516–44523, https://doi.org/10.1039/C5RA03731J.

25. G. W. Ewing, *Instrumental Methods of Chemical Analysis* (Buchler, 2013).

26. L. S. S. M. Magalhães, D. B. Andrade, R. D. S. Bezerra, et al., "Nanocomposite Hydrogel Produced From PEGDA and Laponite for Bone Regeneration," *Journal Functional Biomaterials* 13, no. 2 (2022): 1–15, https://doi.org/10.3390/jfb13020053.

27. A. Selim, A. J. Toth, D. Fozer, K. Suvegh, and P. Mizsey, "Facile Preparation of a Laponite/PVA Mixed Matrix Membrane for Efficient and Sustainable Pervaporative Dehydration of C1–C3 Alcohols," *ACS Omega* 50, no. 2 (2020): 32373–32385, https://doi.org/10.1021/acsomega.0c04380.

28. G. M. C. Alwis, N. Kottegoda, and U. N. Ratnayake, "Facile Exfoliation Method for Improving Interfacial Compatibility in Montmorillonite-Natural Rubber Nanocomposites: A Novel Charge Inversion Approach," *Applied Clay Science* 191 (2020): 1–8, https://doi.org/10.1016/j.clay.2020.105633.

29. V. J. Santos, "Master Dissertation," (2019) Síntese e Caracterização de Hidrogéis de Poli (n-vinil-2-pirrolidona) Contendo Nanoprata e Argila Laponite RD Para Modulação da Liberação de Neomicina.

30. M. B. El-Arnaouty, M. Eid, M. Salah, and E. A. Hegazy, "Preparation and Characterization of Poly Vinyl Alcohol/Poly Vinyl Pyrrolidone/Clay-Based Nanocomposite by Gamma Irradiation," *Journal of Macromolecular Science* 49 (2012): 1041–1051, https://doi.org/10.1080/10601325.2012.728466.

31. F. Ullah, M. B. H. Othman, F. Javed, Z. Ahmad, and H. M. Akil, "Classification, Processing and Application of Hydrogels: A Review," *Materials Science and Engineering: C* 57 (2015): 414–433, https://doi.org/10.1016/j.msec.2015.07.053.

32. S. Wang, Y. Hu, L. Song, Z. Wang, Z. Chen, and W. Fan, "Preparation and Thermal Properties of ABS/Montmorillonite Nanocomposite," *Polymer Degradation and Stability* 77, no. 3 (2002): 423–426, https://doi.org/10.1016/S0141-3910(02)00098-8.